

Phase Vortices in Charge Density Wave
Condensate

Kazumi Maki

Department of Physics

University of Southern California

Los Angeles, California 90089-0484

In the sliding CDW regime a sheet of phase vortices are formed at the boundary of two sliding CDW domains with different sliding velocities. This sheet of vortices move parallel to the boundary with the average velocity determined by the difference of the sliding velocities. This sheet of vortices give rise to both the dc and the ac current.

As is well known a number of quasi-one dimensional charge density wave (CDW) systems like NbSe₃ and TaS₃ (orthorhombic and monoclinic) exhibit nonOhmic conduction when the applied electric field exceeds the threshold field E_T of the order of 10^{-2} - 1 Volt cm^{-1} . More intriguing is the appearance of the narrow band noise (a series of peaks at harmonically related frequencies seen in the spectrometer) in the nonOhmic regime.¹⁻⁴ As to the nonOhmicity, it is generally believed that the extra current above E_T is due to the charge transport of the sliding CDW. Since the extra charge associated with the CDW is given by

$$\rho_1(\vec{r}) = n_c(T) \cos(Qx + \phi) \quad (1)$$

with $Q=2k_F$ and the chain direction is taken as the x axis, the sliding of the CDW with velocity v accounts for the linear relation

$$J_{CDW} = en_c v = en_c \omega Q^{-1} \quad (2)$$

established by Monceau et al.² Furthermore the observed n_i^2 dependence⁵ of E_T is consistent with the impurity pinning of the CDW⁶, where n_i is the impurity concentration.

As to the origin of the narrow band noise a variety of models have been proposed. The most popular one is the classical washboard model,⁷⁻⁹ where the phase of the CDW behaves like a classical particle in a periodic potential,

$$\eta \dot{\phi}_t + \omega_0^2 \sin \phi = \frac{e}{\pi M} E \quad (3)$$

where η is the damping coefficient, ω_0 is the pinning frequency and M is the

mass of the CDW. From the microscopic phase Hamiltonian one can derive Eq.(3), 1) if one ignores the spatial dependence of ϕ and 2) if the periodic potential is assumed to be a simple cosine function. The replacement of the inertia term by the viscous term may be justified from the experimental fact that the CDW behaves in the ac field like an overdamped oscillator.

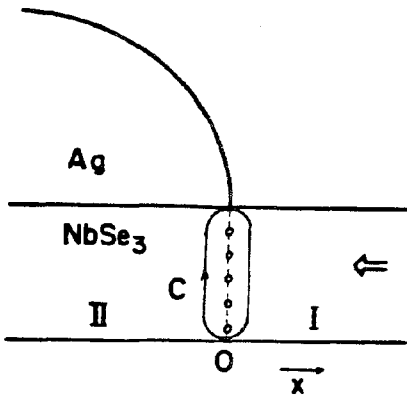
Although this model can describe the coarse features of the nonOhmic conductivity; 1) the existence of the threshold field E_T and 2) appearance of the ac current for $E > E_T$, it is too crude to describe the details of the nonlinear conductivity. In particular, Eq.(3) predicts the square root increase of the dc current as $(E - E_T)^{\frac{1}{2}}$, which has never been observed.

Furthermore the ac current has definite frequencies. In any case by the assumption 1) large degrees of freedom associated with ϕ are completely disregarded. It is quite natural therefore to improve the model by introducing more degrees of freedom in the problems. This possibility has been pursued into two different directions by Sneddon et al.¹⁰ and by Pietronero and Strässler.¹¹ The vortex model may be considered as the third way to salvage this unused degrees of freedom. Furthermore the

vortex model can avoid difficulties, which beset the classical washboard model.¹² First of all we shall draw attention to the fact that the contacts on the NbSe₃ sample in general give rise to an enormous perturbation on the sample.¹² This is readily seen in Fig. 1. Since the contact provides a large shortening path, we expect that the local electric field immediately below the contact is much smaller

Fig.1 The sample geometry at the contact (silver paint) is schematically shown. The current flows in the -x direction. The open circles are an array of vortices moving in the y direction.

than that in the bulk; $E_{II} \ll E_I$ where the region II is under the contact and the region I is the outside of this region. In the following we shall consider a typical case $E_I = E > E_T$ while $E_{II} = 0$. Strictly speaking there is a transition region of width of λ_{TF} between the region I and II, where the electric field changes from $E=0$ to E_T . However this Thomas-Fermi length λ_{TF} is much smaller than ξ ($\approx 10^2 \text{ \AA}$) the coherence length of the CDW condensate. Therefore we can assume for practical purpose that the electric field changes abruptly from E to 0 at the boundary. When $E > E_T$ in the region I, the CDW in the region I is sliding with velocity v uniformly in the -x direction. On the



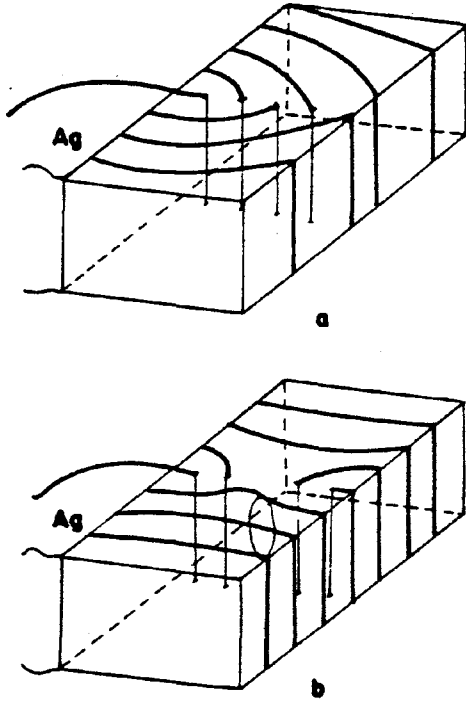


Fig.2 Two possible configurations of vortices are shown a) asymmetrical and b) symmetrical. The thick curves are the crest of the CDW.

difference in the sliding velocities of two domains as

$$2\pi \langle v n_v \rangle = Q(v_1 - v_2) \quad (4)$$

which is nothing but the conservation of the phase as well as the conservation of the dc component of the CDW current J_{CDW} in the x-direction.

In order to describe the phase vortex in the CDW we need the phase Hamiltonian;

$$H = \frac{1}{2} N_0 \int d^3x \vec{\partial}\phi \vec{c}^2 \vec{\partial}\phi + \int d^3x V(\phi) \quad (5)$$

where N_0 is the density of state at the Fermi level, \vec{c}^2 is the squared phase velocity tensor (Note that the system is quite anisotropic) and $V(\phi)$ is the impurity potential which pins the phase oscillation. In the following we shall invoke the potential term only through the Lee-Rice length⁶, which provides a natural screening distance for the local phase disturbance.

other hand in the region II the CDW is immobile implying that there is a clash of the CDW at the boundary of I and II. As is well known in other examples in condensed matter physics, this clash is most economically avoided by introducing a sheet of phase vortices, which moves transversally to the progressing CDW. Two possible vortex configurations are shown in Fig.2 a) and b). Therefore in real experiments with NbSe₃ sample as shown in Fig. 1, appearance of a sheet of vortices are unavoidable.

More generally, if two phase domains sliding with different velocities share a boundary, the boundary contains necessarily an array of phase vortices moving along the phase boundary transverse to the sliding domains.

The average of the product of the vortex velocity and the linear vortex density n_v is determined by the

Following Lee and Rice⁶ we introduce a new length units by $y' = \frac{C_1}{C_2} y$ and $z' = \frac{C_1}{C_3} z$ into Eq.(5). Then in terms of y' and z' Eq.(5) is rewritten as

$$H = \frac{1}{2} N_0 C_2 C_3 \int d^3x (\nabla\phi)^2 + C_2 C_3 C_1^{-2} \int d^3x V(\phi) \quad (6)$$

A vortex line sits at $x=0$ and $y=0$ and parallel to the z axis is given by

$$\phi = \tan^{-1} (y/x) \quad (7)$$

Substituting this into Eq.(6), the vortex energy per unit length (now measured in z rather than in z') is given by

$$\epsilon_V = \pi N_0 C_1 C_2 \ln \left(\frac{\lambda}{\xi} \right) \quad (8)$$

where we have cut off the logarithmic divergence at ξ the BCS coherence length and λ the Lee-Rice length. The coefficient of the logarithm may be rewritten as $\pi N_0 \Delta^2 \xi \xi_2$, with $\xi_2 = C_2 C_1^{-1} \xi$. Therefore ϵ_V is comparable to the condensation energy associated with an ellipse with an area $\pi \xi \xi_2$. When there are two vortices at $(0, y_1)$ and $(0, y_2)$, we have

$$\phi = \tan^{-1}(y-y_1/x) + \tan^{-1}(y-y_2/x) \quad (9)$$

Substituting this into Eq.(6), we obtain the interaction energy of two vortices per unit length as

$$\epsilon_I = \pi N_0 C_1 C_2 \ln(\lambda/|y_1-y_2|) \quad (10)$$

where we assumed that $|y_1-y_2| \ll \lambda$. Making use an analogous analysis in the case of superconductivity, Eq.(10) may be generalized as

$$\epsilon_I = \pi N_0 C_1 C_2 K_0 \left(\frac{|y_1-y_2|}{\lambda} \right) \quad (11)$$

where $K_0(z)$ is the modified Bessel function. In the limit $|y_1-y_2| \ll \lambda$, Eq.(11) reproduces Eq.(10) while for $|y_1-y_2| \gg \lambda$, the interaction potential decay exponentially with the distance $|y_1-y_2|$.

Now we shall consider an array of vortices at $x=0$ and $y=y_i(t)$. The corresponding ϕ is given by

$$\phi = \sum_i \tan^{-1} (y-y_i(t)/x) \quad (12)$$

To determine the equilibrium positions $\{y_i\}$ is a difficult task even in the absence of the electric field, as we have to take into account of the image force, which attracts the vortices near the surfaces ($y=0$ and $y=L$ in the

present geometry). Therefore we believe that the vortices are more dense near $y=0$ and $y=L$ even in the absence of an electric field which causes sliding of the CDW in the region II. When there is a discontinuity of ϵ in the electric field at $x=0$, as shown in Fig. 1, the electric field introduces an additional potential energy which pushes the vortex in the y direction. This energy is evaluated from

$$\epsilon_E = \frac{e}{\pi} \int_0^\lambda dx \int_0^L dy \epsilon \phi \quad (13)$$

For a vortex at $y=y_i$, Eq.(13) gives

$$\begin{aligned} \epsilon_E &= \frac{e}{\pi} \int_0^\lambda dx \int_0^L dy \epsilon \tan^{-1} \left(\frac{y-y_i}{x} \right) \\ &= \frac{e}{\pi} \epsilon \left\{ \frac{1}{4} \left[(L-y_i)^2 \ln \left[\left(\frac{\lambda}{L-y_i} \right)^2 + 1 \right] - y_i^2 \ln \left[\left(\frac{\lambda}{y_i} \right)^2 + 1 \right] \right] \right. \\ &\quad \left. + \lambda \left((L-y_i) \tan^{-1} \left(\frac{L-y_i}{\lambda} \right) + y_i \tan^{-1} \left(\frac{y_i}{\lambda} \right) \right) \right. \\ &\quad \left. + \frac{3}{4} \lambda^2 \left[\ln(\lambda^2 + (L-y_i)^2) - \ln(\lambda^2 + y_i^2) \right] \right\} \\ &= \frac{e}{2\pi} \epsilon (L^2 - 2Ly_i) \ln(\lambda/L) \end{aligned} \quad (14)$$

Therefore for $\lambda \gg L$, the electric field provides a linear potential for a vortex at $y=y_i$. Let us assume that the electric field sets the array of vortices in motion. This array of vortices generate both the dc and the ac current in the x direction, which is given by

$$J_{CDW} = en_c Q^{-1} \dot{\phi}_t \quad (15)$$

We shall come back to Fig. 1, where open circles are vortices moving in the y direction along the line $x=0$. We are interested in the difference in the CDW currents in the regimes I and II, which can be obtained by integrating Eq.(15) along the path C, which encloses all the vortices

$$\begin{aligned} \Delta J &= J_{CDW2} - J_{CDW1} \\ &= en_c Q^{-1} \oint_C d\ell \dot{\phi}_t \end{aligned} \quad (16)$$

Substituting Eq.(12) into Eq.(16), we find

$$\Delta J = -2\pi e n_c Q^{-1} \sum_i \dot{y}_i \quad (17)$$

where \dot{y}_i is the velocity of the vortices. If we take the time average of

Eq.(17), the dc component of Eq.(17) is nothing but the minus of the difference in J_{CDW} given by Eq.(2) for two regimes. The vortex sheet compensates exactly the missing dc component of the CDW current. On the other hand, since the motion of vortices cannot be uniform, Eq.(17) can generate the ac component. The appearance of the ac component associated with the moving vortex sheet is also consistent with a recent experiment¹³, which indicates that the noise source is highly localized near the contacts.

There are a few mechanisms, which break the uniform motion of an array of vortices; the sample walls where the vortex enters and exits give rise to pinning potentials in the case shown in Fig. 2 a), while the creation of vortex ring at the center of the sample is also a discontinuous event in the case shown in Fig. 2 b). In addition to these intrinsic effects, crystalline defects in the vortex path will provide a pinning potential for a vortex. In general, when a vortex is approaching the pinning potential, the velocity increases above the average velocity, takes the maximum value at the center and then falls to the average velocity as the vortex moves away from the center. This will show up as regular solitonic peaks in $J_{CDW}(t)$. Furthermore the effect is quite visible if the total vortex number in the array is not so large. Although the absolute magnitude of the solitonic structure is not affected as the vortex number increases, the more incoherent behavior of other vortex will wash out this feature when the vortex number is increased. The above solitonic feature is consistent with some of the experimental observations.¹²

The broad band noise is also very likely generated by random motion of the array of vortices. However, in order to obtain more explicit expression of $J_{CDW}(t)$ for example a further theoretical analysis is required.

Acknowledgement

The notion of an array of vortices is formed while discussing with Phuang N. Ong on his experimental data on NbSe₃ sample. I thank Phuan Ong for discussing both theoretical and experimental aspects of the model. Present work is supported by the National Science Foundation under grant number DMR-82-14525.

References

1. R.M. Fleming and C.C. Grimes, Phys. Rev. Lett. 41 1423 (1977); R.M. Fleming, Phys. Rev. B22 5606 (1980).
2. P. Monceau, J. Richard, and M. Renard, Phys. Rev. Lett. 45 43 (1980); Phys. Rev. B25 931 (1982).

3. G. Grüner, A. Zettle, W.G. Clark and A.H. Thompson, Phys. Rev. B23 6813 (1981).
4. K. Hasegawa, A. Maeda, S. Uchida, and S. Tanaka, Sol. Stat. Comm. 44 881 (1982).
5. N.P. Ong, J.W. Brill, T.C. Eckert, J.W. Savage, S.K. Khanna, and R.B. Somoano, Phys. Rev. Lett. 42 811 (1979).
6. P.A. Lee and T.M. Rice, Phys. Rev. B19 3970 (1979).
7. G. Grüner, A. Zawadowski, and P.M. Chaikin, Phys. Rev. Lett. 46 511 (1981).
8. P. Monceau, J. Richard, and M. Renard, Phys. Rev. B25 931 (1982).
9. J. Richard, P. Monceau and M. Renard, Phys. Rev. B25 948 (1982).
10. L. Sneddon, M.C. Cross, and D.S. Fisher, Phys. Rev. Lett. 49 292 (1982).
11. L. Pietronero and S. Strässler, preprint.
12. N.P. Ong, G. Varma, and K. Maki, to be published.
13. N.P. Ong and G. Verma, Phys. Rev. B27 4495 (1983).